

AN XMM-NEWTON VISION OF THE NGC 2023 CLUSTER AND ITS SURROUNDINGS

M. A. López-García¹, J. López-Santiago¹, J. F. Albacete-Colombo², E. De Castro¹

¹ Universidad Complutense de Madrid, Dept. de Astrofísica, Facultad C.C. Físicas, Madrid, Spain

² Centro Universitario Regional Atlántica (CURZA) Universidad Nacional del COMAHUE, Monseñor Esandi y Ayacucho, Viedma (Rio Negro), Argentina

Abstract The southern part of the Orion B giant molecular cloud complex, L 1630, borders the large H II region, which is expanding into the molecular cloud. The interface between the molecular cloud and the HII region (IC 434) is seen as a bright ridge with the Horsehead Nebula and several smaller pillars on it. NGC 2023 is a molecular cloud situated at approximately 30 arcmin at the East of the ridge, where star forming is taking place actively. This region contains molecular clumps detected in the millimetric range where stars are just forming. We have used data from the archive of the XMM-Newton mission to look for differences in the X-ray properties of these objects. We present our results with special attention to an obscured X-ray source detected by the VLA in the millimetrics and by Spitzer in the IR.

Observation The observation was performed on a single exposure of 30 ks on 2002 March in revolution 419. The European Photon Imaging Cameras (EPIC) were centred at R.A. = 05h41m47.20s and Dec. = 02d16m37.0s. High background periods were removed from the event list. The effective exposure time was reduced to approximately the half (see Table 1).

	PN	MOS1	MOS2
Exposure Time (ks)	25.09	29.13	29.12
Useful Exposure Time (ks)	13.60	15.00	15.80
Filter	Medium	Thin	Medium
Mode	Extended Full Frame	Full Frame	Full Frame

Table 1: General parameters of the XMM-Newton observations.

Source Detection We used the SAS task *edetect_chain* to detect the sources of the FOV, using images in different energy bands in PN, MOS1 and MOS2 with the standard threshold. A total of 50 sources were detected. We discarded 14 of them, clear multiple or spurious detections close to the detector border. The flux was determined using a conversion factor (CF) between count-rate and flux $CF = 2.87 \times 10^{-12} \text{ erg ph}^{-1}$. This factor was obtained from spectral fitting of large count-rate sources of the observation.

X-Ray Properties We analysed the spectra of the sources using a 2-Temperature model using XSPEC with the hot plasma model APEC/APED and absorptions from WABS.

Name	NH ($\times 10^{22} \text{ cm}^{-2}$)	kT_1 (keV)	kT_2 (keV)	Z (Z_{sun})	Unabsorbed f_x ($\times 10^{-13} \text{ erg cm}^{-2} \text{ s}^{-1}$)	Log L_x (erg s^{-1})
MIR31	0.00	0.62	1.26	0.20	3.99	2.18×10^{31}
MIR46	1.31	11.61	---	4.99	1.38	5.42×10^{29}
MIR52	0.66	1.18	5.22	0.18	14.70	1.43×10^{31}
MIR60	0.19	0.11	1.04	0.31	0.57	1.21×10^{30}
MIR71	0.10	0.80	2.68	0.4	1.82	7.09×10^{30}
MIR76	0.77	9.30	---	5.0	2.27	9.91×10^{29}
MIR80	0.38	1.02	10.40	0.08	20.65	3.36×10^{31}
Name_4	0.08	2.36	---	0.18	11.67	3.65×10^{31}
Name_7	0.05	0.34	1.21	0.12	3.19	1.13×10^{31}
Name_8	1.00	0.76	5.93	0.22	4.13	9.26×10^{30}
Name_10	1.18	0.13	3.20	0.00	4.11	6.80×10^{30}
Name_12	0.23	1.96	---	0.09	2.14	4.38×10^{30}

Table 2: Spectral parameters of the NGC2023 sources with high statistic of photons

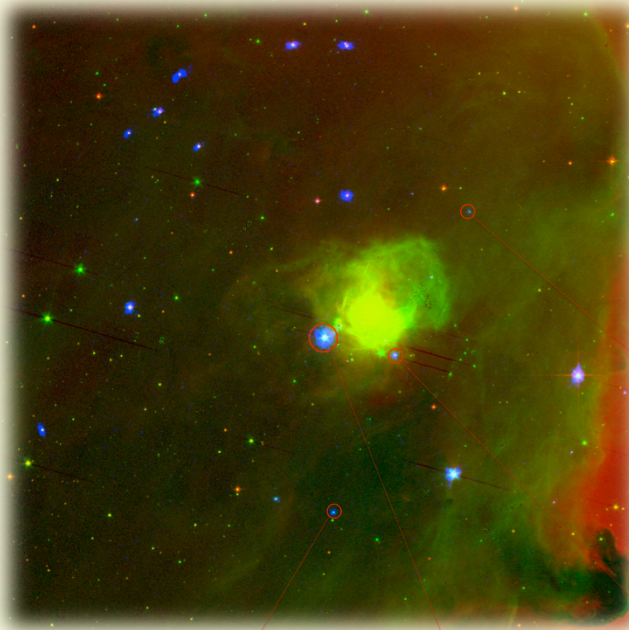


Fig. 1: RGB image of the NGC 2023 regio. Red: Optica, Green: Mid-infrared and Blue: X-ray.

Interesting Sources

MIR76: It is highly absorbed and presents the iron XXV line at 6.7 keV.

MIR80: The brightest X-ray source of the region.

MIR60: Classified as a Class II. The star is associated with a HH object.

MIR46: A probable class I with Spitzer counterpart, but no 2MASS.

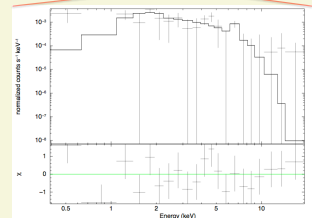
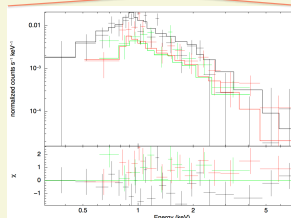
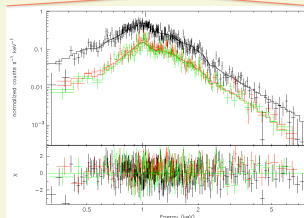
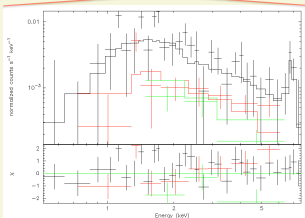


Fig. 2, 3, 4 and 5: X-ray spectra. Black is for EPIC-pn, red and green are for EPIC-mos. The best fit to each spectrum is plotted. The bottom panel shows the deviation of the model from the observed spectra in each spectral bin.

REFERENCES

- López-Santiago et al. 2010, A&A, 524, A97
- Mookerjee et al. 2009, A&A, 507, 1485
- Robitaille et al. 2007, ApJS, 176, 256
- Robrade et al. 2005, A&A, 435, 1073

ACKNOWLEDGMENTS

This work is supported by the Spanish Ministerio de Ciencia e Innovación under grant AYA2008-06423-C03-03 and by grant PICT 2007-02177 (Secyt, Argentina).

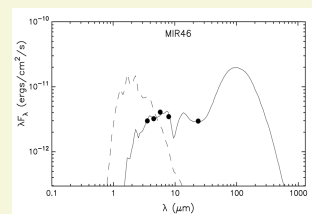
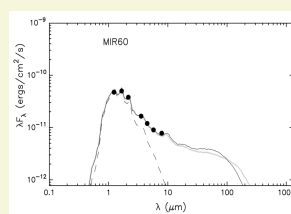
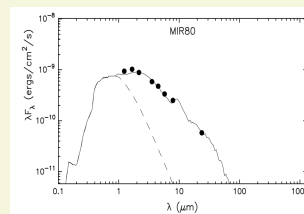


Fig. 6, 7 and 8: Infrared SEDs. The filled circles show the input fluxes. The black line shows the best fit, and the gray lines show subsequent good fits. The dashed line shows the stellar photosphere corresponding to the central source of the best-fit model, as it would look in the absence of circumstellar dust (but including interstellar extinction). The model was obtained in <http://caravan.astro.wisc.edu/protostars/> following Robitaille et al 2007.